MDPI

Article

Scour at a Submerged Square Pile in Various Flow Depths under Steady Flow

Shengtao Du [1], Guoxiang Wu [2,*], Bingchen Liang [3], David Z. Zhu [1] and Risheng Wang [4]

[1] School of Civil and Environmental Engineering, Ningbo University, Ningbo 315211, China; dushengtao@nbu.edu.cn (S.D.); david.zhu@ualberta.ca (D.Z.Z.)

[2] College of Engineering, Ocean University of China, Qingdao 266100, China

[3] Shandong Provincial Key Laboratory of Ocean Engineering, College of Engineering, Ocean University of China, Qingdao 266100, China; bingchen@ouc.edu.cn

[4] College of Civil Engineering, Shandong Jiaotong University, Jinan 250357, China; wangrsh2004@163.com

* Correspondence: guoxiang@ouc.edu.cn

Abstract: Local scour around submerged piles in currents are common in coastal and offshore engineering. This paper studies the influences of the submergence ratio (flow depth to pile height) on local scour around a square pile in steady flow. Submergence ratio ranging from 1–4, as well as two unsubmerged tests, were tested with a 10×10 square pile of 20 cm height. The three-dimensional profiles were measured to study the scour and deposition characteristics. Results show that the maximum scour depth was always at the upstream corner points rather than at the symmetry center point of the pile. The temporal maximum scour depth achieved its equilibrium sate in less than 4 h for each test. The equilibrium scour depths at the upstream corner points were independent of the submergence ratio when the latter was larger than 1.5. These findings give meaningful reference to the numerical simulations and local scour depth protections in the submerged pile cases deeper than which the flow depth does not affect the equilibrium scour depth.

1. Introduction

In coastal and offshore engineering, local scour induced by currents threatens the stability of structures. Numerous researchers have focused on the local scour of unsubmerged circular piles [1–5], but studies on submerged square piles are few. The submerged vertical square piles represent a range of sub-sea structures, such as caissons, manifolds and pipeline foundations in oil and gas explorations [6]. It is known that the flow depth (h) to pile height (h_c) ratio (h/h_c) has a potential effect on the mean and turbulent bulk statistics at the upstream and downstream of a submerged cube [7]. According to the experimental tests in Shamloo et al. [8], the ratio of flow depth to hemisphere height affected the flow patterns; as a result, the sediment scour and sand dunes around the hemispheres were quite different with these various ratios. Therefore, the submergence ratio of h/h_c plays an important role in the characteristics of local scour.

The strong, nonlinearly complex interactions of fluid, pile and sediments induced by the flow turbulence of the horseshoe vortex, flow accelerations and wake vortices around the pile are the mechanisms of local scour [9]. In addition to the experimental methods in studying the mechanisms and characteristics of local scour that were conducted by [1–9], recently, Baykal et al. [10] studied the bed shear stress induced by these three phenomena in waves and currents numerically. Specifically, they found that in accordance with the current conditions alone, the horseshoe vortex underwent substantial changes in waves depending on the Keulegan–Carpenter number. Afzal et al. [11], Gazi and Afzal [12] and Gautam et al. [13] applied the Level-Set method to a three-dimensional computational fluid dynamics model to study the formation process of vortices around the pier in waves,

currents or combined waves and currents. While Liang et al. [3], Yang et al. [4], Yao et al. [7] and Roulund et al. [9], obtained the equilibrium scour depth by adapting the temporal scour depth data to curves, Cheng et al. [14], Gazi and Afzal [15] and Gazi et al. [16] derived the equilibrium scour depth equations on the concept of the volume of sediment transport and flow turbulence energy through mathematical analysis methods.

A few studies have discussed the effects of pile heights on local scour in fixed flow depths in submerged conditions. Dey et al. [17] conducted experimental tests to study local scour around submerged circular piles. A coefficient that represents the ratio of equilibrium scour depth of a submerged cylinder to that of an unsubmerged cylinder with the same diameter was proposed. Zhao et al. [18] simulated the flow fields with a finite element numerical model and found that the near bed shear stress of the higher pile was related to a larger and wider horseshoe vortex. Based on the pile Reynolds number, Euler and Herget [19] estimated the equilibrium scour depth with flow depth ranging from 2.1 cm to 10.1 cm. Later, Zhao et al. [20] experimentally studied rectangular and square piles with the pile height to width (D) ratios of 0.25 to 1.0. They found that the equilibrium scour depth increased with the increasing pile height in submerged conditions. Yao et al. [6] designed a wide range of $h_c/D \leq 1$ for both circular and square piles, most of which were experimented upon from nearly live-bed scour to sheet flow conditions. Their results show that the equilibrium scour depth reduced with the flow depth to pile width (h/D) when $h/D \leq 4$.

However, these above studies, in which the pile height and flow depth were variable and constant values, respectively, probably cannot reflect the real effects of flow depth on local scour, because the scour depth increased significantly with the increasing pile height [21]. For these reasons, this paper aims to study the influences of flow depth on local scour at a submerged square pile in clear-water scour conditions with various flow depths. The focus is on the temporal scour depth, the equilibrium scour depth and bed profiles.

2. Methodology

2.1. Temporal and Equilibrium Scour Depth Predictions

The bed shear stress (τ_0) is the frictional force exerted on a unit area of the bed by the current flowing over it [22]. It is made up from contributions due to the skin friction, the form drags and a sediment transport. The critical shear stress (τ_{cr}) is the minimum shear stress to induce a sediment incipient motion at the bed. In a flat bed, the dimensionless shear stress is equal to Shields number (θ), which is caused by the skin friction when the bed is immobile. As the bed shear stress is related to the depth averaged flow velocity (U), the square root of Shields number to critical Shields number (θ_{cr}), i.e., $(\theta/\theta_{cr})^{0.5}$, was considered to be flow intensity [2]. These relationships were in the following Equations (1)–(3):

$$\tau_0 = \rho C_D U^2 \tag{1}$$

$$\theta = \frac{\tau_0}{(\rho_s - \rho)g d_{50}} \tag{2}$$

$$\theta_{cr} = \frac{0.30}{1 + 1.2 D_*} + 0.055[1 - \exp(-0.02 D_*)] \tag{3}$$

where ρ is water density, $C_D = \left[\frac{\kappa}{1+\ln(z_0/h)}\right]^2$ is the coefficient, $\kappa = 0.4$ is von Karman's constant, z_0 is the roughness height due to skin friction, ρ_s is sediment density, g is acceleration due to gravity, d_{50} is median sediment particle size, $D_* = [g(s-1)/\nu^2]^{1/3} d_{50}$ is non-dimensional sediment particle size, ν is kinematic viscosity of water, $s = \rho_s/\rho$ is the specific gravity of sediments.

For unsubmerged piles, Equation (4) is widely used in predicting temporal scour depth $d_s(t)$ at time t [2,4,6]:

$$d_s(t) = d_{se}[1 - exp(-t/T)] \tag{4}$$

where $d_s(t)$ and the equilibrium scour depth d_{se} were measured at the upstream symmetry center point for circular piles, $T = \frac{D^2}{[g(s-1)d_{50}^3]^{0.5}} T^*$ is time scale, $T^* = \frac{\delta}{2000D} \theta_s^{-2.2}$ is a non-dimensional time scale proposed by Sumer et al. [23], δ is boundary layer thickness.

It is apparent that Equation (4) cannot estimate the equilibrium scour depth without conducting a scouring test. Thus, an empirical formula from Melville [1] was modified to adapt to the cases in submerged square piles. On one hand, because the maximum scour depths were located at K_M for square piles [24], a submergence factor K_{hh_c} that represents the flow depth influence on equilibrium scour depth was introduced into the empirical formula. As seen in Equation (5), a new factor of K_{hh_c} was added to the equation from [1].

$$d_{se} = K_{hh_c} K_{hD} K_I K_d K_s K_\alpha K_G \tag{5}$$

where K_{hh_c} is the factor for submergence, K_I is the flow intensity factor in submerged square piles, K_d is the sediment size factor, K_s is the pile shape factor, K_α is the factor for flow attacking angle, K_G is the factor for the channel geometry.

2.2. Experiments Setups

Experiments were conducted in the Hydraulic Modeling Laboratory at ShanDong Jiao-Tong University, China. The flume was 60 m long, 1.2 m wide and 1.5 m deep. The test section was located in the middle of the flume, as shown in Figure 1a. Water was pumped from left to right and was circled by a pipe outside of the flume. The sand bed was 8.4 m long, 1.2 m wide and 0.2 m height. Scour depths at upstream corner points (K_M, i.e., $x/D = -0.5, y/D = \pm 0.5$), upstream symmetry center point (K_C, i.e., $x/D = -0.5, y/D = 0$), as shown in Figure 1b, were observed with scouring time, respectively. The medium grain size of sand was 0.65 mm and the geometric standard deviation $\sigma_g = (d_{85}/d_{15})^{0.5}$ was 1.27. The specific gravity of sediment grain density is 2.65 and the porosity is 0.4. Calculated with equation $\tan(\alpha_d) = 0.74 d_{50}^{0.05}$ from Cheng and Zhao [25], the angle of static repose α_d was 36° under water.
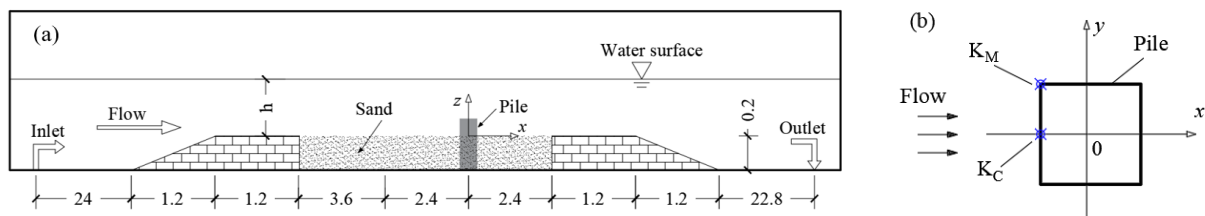
Figure 1. Test flume and coordinate system modified from Du and Liang [24], unit: m, (**a**) Side view of the flume, (**b**) Sketch view of K_M and K_C points.

Both of the flow velocity and scour depth were measured by using a Nortek Vectrino II Acoustic Doppler Velocimeter (ADV) with their accuracies of ±0.1 mm/s and ±1 mm, respectively. The flow velocity at each point was measured where the pile model would be settled and was averaged for a period of 5 min, with a sampling frequency of 20 along the flow depth. Scour depths at K_M and K_C were measured by the distance function of the ADV. The bed elevations were measured by a Seatek, which is a topographic measuring instrument with 32 transducers, without draining out the water. The measuring accuracy and diameter of each transducer were ±0.1 mm and 1 cm, respectively.

Experimental tests are listed in Table 1. The depth averaged flow velocity (U) ranged from 17.2 cm/s to 23.0 cm/s. The flow intensity $(\theta/\theta_{cr})^{0.5}$ was kept at a constant value of 0.55. The Froude number ($Fr = U/\sqrt{gh}$) and Reynolds number ($Re_D = UD/\nu$) ranged from 0.08–0.17 and 1.7×10^4–2.3×10^4, respectively. For unsubmerged cases of Test A1, flow depth (h) was kept 10 cm. For submerged cases of Tests A3–A7, flow depth ranging from 30 cm to 80 cm corresponded to the submergence of $h/h_c = 1 - 4$. The transitional flow depth in Test A2 was equal to the pile height. The scouring duration (t_d) was 9 h.

d_M and d_C were scour depths at K$_M$ and K$_C$, respectively, measured at the end of the experiment t_d.

Table 1. Tests for the influences of flow depths.

Test	h (cm)	h/h_c	U (cm/s)	Fr	$(\theta/\theta_{cr})^{0.5}$	t_d (h)	d_M(cm)	d_C(cm)
A1	10	0.5	17.2	0.17	0.55	9	2.1	0
A2	20	1.0	18.9	0.14	0.55	9	2.3	0.7
A3	30	1.5	20.0	0.12	0.55	9	2.8	1.2
A4	40	2.0	20.4	0.10	0.55	9	2.9	1.3
A5	50	2.5	21.6	0.10	0.55	9	2.8	1.7
A6	70	3.5	22.5	0.09	0.55	9	2.9	2.0
A7	80	4.0	23.0	0.08	0.55	9	2.9	2.2

3. Tests Results and Discussion

3.1. Temporal and Equilibrium Scour Depths

To study the influences of flow depth on local scour, unsubmerged (Test A1), transitional Test A2 and submerged cases of Test A3–A7 were investigated. In the process of these tests, scour depths at K$_M$ were observed much deeper than those at K$_C$ (see Table 1). These differences are probably owed to the larger bed shear stress at K$_M$ than at K$_C$, as Roulund et al. [9] found that the bed shear stress at the upstream lateral side of the pile was 7 times that of the symmetry upstream of the pile in a numerical simulation test with the Froude number of 0.14. Thus, scour always started at the upstream corners of the pile in clear-water scour conditions [20,24]. Because the scour depth evolution trends at K$_M$ and K$_C$ were similar, scour depths at K$_M$ were discussed as an example. As presented in Figure 2a, each test was carried out for 9 h to get its equilibrium scour state at K$_M$. The scour depth evolution curves appeared to be asymptotic, i.e., scour depths increased rapidly in the initial scouring phase, slowed down in the developing phase, and kept at a constant value in the equilibrium scouring phase.

(**a**) Temporal scour depths at K$_M$ (**b**) Equilibrium scour depths at K$_M$ and K$_C$
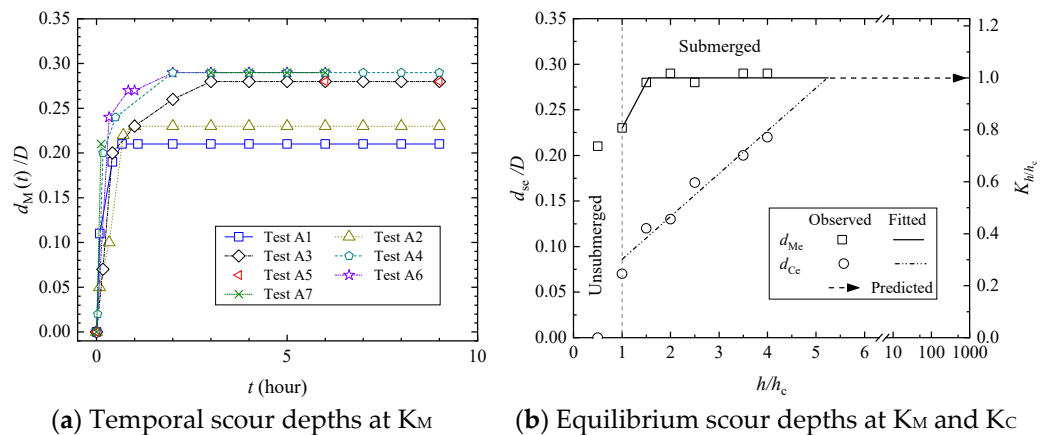
Figure 2. Scour depths of Tests A1–A7. $d_M(t)$ is the scour depth at scouring time t at K$_M$, d_{se} is the equilibrium scour depth at K$_M$ (d_{Me}) or K$_C$ (d_{Ce}), K_{hh_c} is the submergence factor on equilibrium scour depths at K$_M$.

In the first 10 min, the relative scour depths of the submerged tests ($d_M(\mathrm{t})/D = 0.2$) were about 2 times those of the unsubmerged case ($d_M(\mathrm{t})/D = 0.1$). Moreover, the duration of developing phase for Tests A3–A7 appeared to be much longer than the unsubmerged case. The unsubmerged Tests A1 and the transitional Test A2 reached their equilibrium states within 1 h, whilst the submerged cases needed 2–4 h. Overall, the equilibrium scour depths were a bit larger than those of the unsubmerged. It seems that the larger the equilibrium scour depth was, the more scouring duration was required for the equilibrium

state. It should be noted that the scour depth evolution of Test A5 was not observed throughout the test. However, as the other tests all reached their equilibrium states in 4 h, the final scour depth of Test A5, which scoured for 9 h, was considered to achieve its equilibrium state as well.

The equilibrium scour depths varied with the submergence ratios, as drawn in Figure 2b. It can be seen that the relative equilibrium scour depth (d_{Me}/D) increased with the submergence ratio (h/h_c) when $h/h_c \leq 1.5$. Once h/h_c is larger than 1.5, the relative equilibrium scour depth was nearly a constant value of 0.29, i.e., its effects on d_{Me}/D is little. This indicates that the bed shear stress induced by the flow accelerations kept a constant value, as Zhao et al. [20] and Baykal et al. [21] found that scour at pile upstream corners was mainly caused by the amplified shear stress that related to flow accelerations. However, scour depth at $\mathrm{K_C}$ was very different. As shown in Figure 2b, the relative equilibrium scour depth (d_{Ce}/D) at $\mathrm{K_C}$ of the unsubmerged Test A1 was zero, whilst d_{Me}/D was 0.21. With the increasing submergence ratio, d_{Ce}/D increased linearly when $h/h_c \leq 4.0$. These characters were the result of the increased relative boundary layer thickness (δ/D) and Re_D that related to the strength of the horseshoe vortex upstream of the pile [9,12].

The gap between d_{Me}/D and d_{Ce}/D tended to decrease and disappear at about $h/h_c = 5$, indicating that the bed shear stress induced by the horseshoe vortex and flow accelerations at $\mathrm{K_C}$ and $\mathrm{K_M}$ [20], respectively, would not increase with flow depth when $h/h_c \geq 5$. Two reasons might be responsible for this phenomenon. One was that there was no bow wave that can reduce the upstream vortex in submerged pile conditions [17]. The other was that the velocity and strength of vortex varied not largely when $Re_D > 10^4$ [12]. Therefore, scour depth at $\mathrm{K_C}$ was thought to increase little when $h/h_c \geq 5$ in the submerged tests.

As the equilibrium scour depth of d_{Me} was always larger than or equal to d_{Ce}, the flow accelerations at pile sides played more important roles in scouring for submerged square piles. Thus, the relationships between the submergence factor of K_{hh_c} and equilibrium scour depth for d_{Me} was estimated (right longitudinal coordinates in Figure 2b). The submergence factor of K_{hh_c} was set to be 1.0 when $h/h_c = 1.5$, larger than which flow depth effects on the equilibrium local scour depth could be ignored. When the pile was submerged in a relatively shallow flow depth, i.e., $1 \leq h/h_c \leq 1.5$, the K_{hh_c} factor, as shown in Equation (6), increased linearly with h/h_c. Therefore, the submergence ratio effects on the equilibrium scour depth was obtained for Equation (5), which was based on the equation proposed by Melville [1].

$$K_{hh_c} = \left\{ \begin{array}{ll} 0.4h/h_c + 0.4 & , \quad 1.0 \leq h/h_c \leq 1.5 \\ 1.0 & , \quad h/h_c > 1.5 \end{array} \right. \tag{6}$$

3.2. Bed Elevation Profiles

To describe the influences of flow depth on sand scour and deposition distributions, examples of three-dimensional topographies, unsubmerged Test A1, transitional Test A2, and submerged Tests A3 and A7, are presented in Figure 3a–d, respectively. They show that the sizes of scour holes upstream and the heights of deposited sands in the lateral sides of the unsubmerged case were much smaller than those of the submerged cases, respectively. The significant erosion behind the pile in transitional Test A2, which was induced by the mixing of separated flow from the top and the separated flow from the sides [8], was much larger than the others. Because the angle of static repose under water is constant for the sand, there is no doubt that a larger scour depth is related to a wider hole. As seen in Figure 3, the scour hole diameters of Tests A1, A2, A3 and A7 were about 0.25D, 0.35D, 0.5D and 0.5D, respectively.
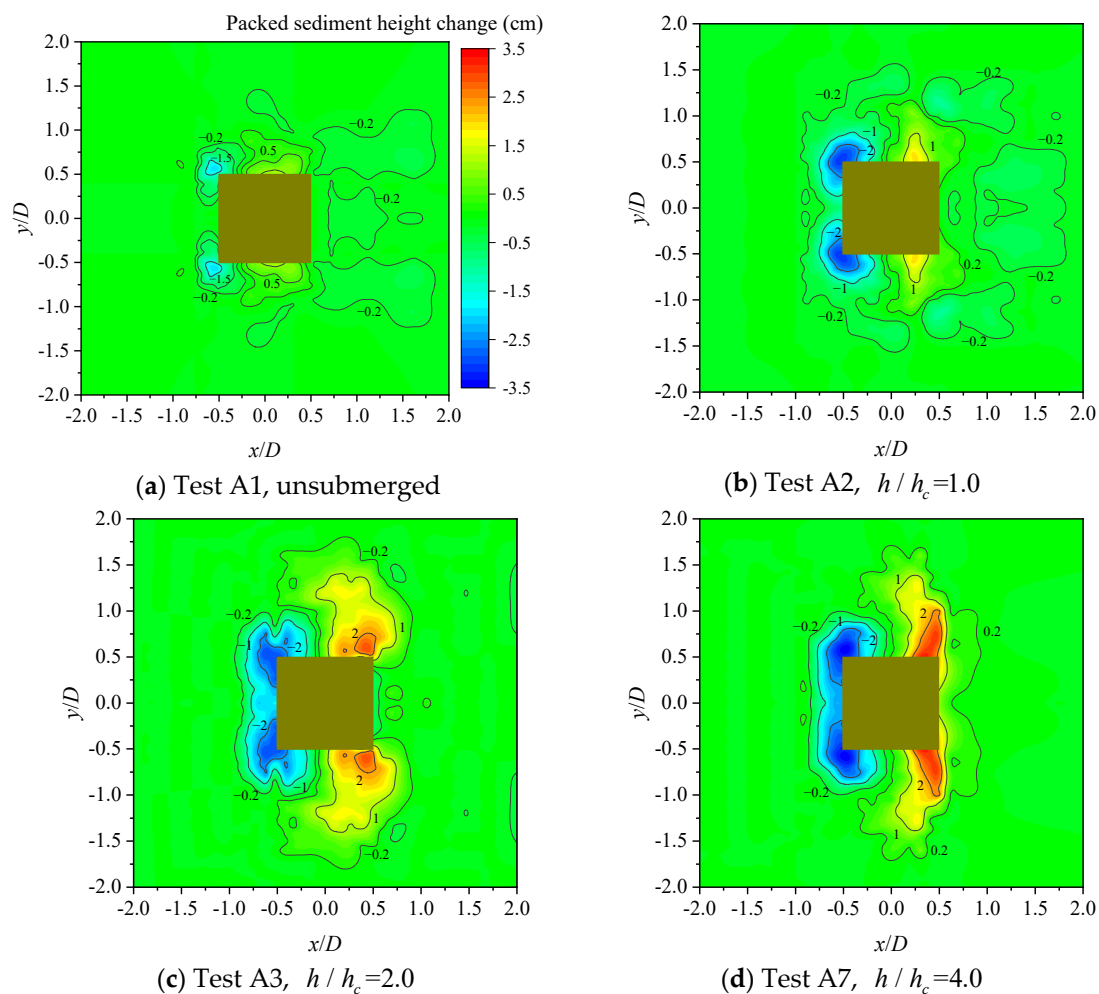
Figure 3. Equilibrium state of topographies of Tests A1, A2, A3, and A7.

With the increasing flow depth, the two separate scour holes upstream extended from upstream corners to the upstream symmetry center line gradually and the scour depth at K_C became deeper simultaneously. These phenomena reflect that both of the depths and sizes of scour holes were governed by the flow accelerations in submerged square piles. Though the bed shear stress had not been measured in these tests, results simulated by Tseng et al. [26] of a square pile show that the bed shear stress at upstream stream corners was more than 4 times that along the upstream symmetry line, which can explain the scour hole spreading process in this paper. With the scour hole depth increased, more sediments were rolled up and transported by flow, resulting in higher and higher deposited sand dunes on the lateral side. Moreover, these sand dunes accumulated with the scour process going on and were moved to the downstream direction gradually by the combinations of wake vortexes and flow.

4. Conclusions

This paper studied the influences of flow depth on local scour around a submerged vertical square pile through experimental tests. Characteristics of sediment scour and deposition were analyzed in various flow depths. The main conclusions can be drawn in the following:

(1) Scour depth at K_C was much smaller than that at K_M when the flow depth to pile height ratio was less than 5. In particular, because of the low flow depth, which related to a weak strength of horseshoe vortex, no sediment scour was found in front of the pile in the unsubmerged test.

(2) The scour depth and height of sediment depositions of the unsubmerged pile were much smaller than those of the submerged cases, respectively. More scouring durations were needed to achieve the scour equilibrium state in the submerged cases than the unsubmerged cases.

(3) Equilibrium scour depth at K_M was independent of flow depth when the flow depth to the pile height ratio was larger than 1.5, while the equilibrium scour depth at K_C increased remarkably with this ratio and became independent of it when the ratio exceeded 5.

(4) The two separate scour holes upstream of the pile were the results of flow accelerations at the upstream pile corners. They were not connected until the flow depth to pile height ratio was 1.5.

References

1. Melville, B.W. Pier and Abutment Scour: Integrated Approach. *J. Hydraul. Eng.* **1997**, *123*, 125–136. [CrossRef]
2. Sumer, B.M.; Fredsøe, J. *The Mechanics of Scour in the Marine Environment*; World Scientific: Singapore, 2002; 536p. [CrossRef]
3. Liang, B.; Du, S.; Pan, X.; Zhang, L. Local Scour for Vertical Piles in Steady Currents: Review of Mechanisms, Influencing Factors and Empirical Equations. *J. Mar. Sci. Eng.* **2020**, *8*, 4. [CrossRef]
4. Yang, Y.L.; Qi, M.L.; Wang, X.; Li, J.Z. Experimental study of scour around pile groups in steady flows. *Ocean Eng.* **2020**, *195*, 106651. [CrossRef]
5. Song, Y.; Xu, Y.; Ismail, H.; Liu, X. Scour modeling based on immersed boundary method: A pathway to practical use of three-dimensional scour models. *Coast. Eng.* **2022**, *171*, 104037. [CrossRef]
6. Yao, W.D.; An, H.W.; Draper, S.; Cheng, L.; Harris, J.M. Experimental investigation of local scour around submerged piles in steady current. *Coast. Eng.* **2018**, *142*, 27–41. [CrossRef]
7. Singh, S.K.; Raushan, P.K.; Debnath, K. Role of multiple flow stages over submerged structure. *Ocean Eng.* **2019**, *181*, 57–70. [CrossRef]
8. Shamloo, H.; Rajaratnam, N.; Katopodis, C. Hydraulics of simple habitat structures. *J. Hydraul. Eng.* **2001**, *39*, 351–366. [CrossRef]
9. Roulund, A.; Sumer, B.M.; Fredsøe, J.; Michelsen, J. Numerical and experimental investigation of flow and scour around a circular pile. *J. Fluid Mech.* **2005**, *534*, 351–401. [CrossRef]
10. Baykal, C.; Sumer, B.M.; Fuhrman, D.R.; Jacobsen, N.G.; Fredsøe, J. Numerical simulation of scour and backfilling processes around a circular pile in waves. *Coast. Eng.* **2017**, *122*, 87–107. [CrossRef]
11. Afzal, M.S.; Bihs, H.; Kumar, L. Computational fluid dynamics modeling of abutment scour under steady current using the level set method. *Int. J. Sediment Res.* **2020**, *35*, 355–366. [CrossRef]
12. Gazi, A.H.; Afzal, M.S. A review on hydrodynamics of horseshoe vortex at a vertical cylinder mounted on a flat bed and its implication to scour at a cylinder. *Acta Geophys.* **2020**, *68*, 861–875. [CrossRef]
13. Gautam, S.; Dutta, D.; Bihs, H.; Afzal, M.S. Three-dimensional Computational Fluid Dynamics modelling of scour around a single pile due to combined action of the waves and current using Level-Set method. *Coast. Eng.* **2021**, *170*, 104002. [CrossRef]
14. Cheng, N.S.; Chiew, Y.M.; Chen, X.W. Scaling Analysis of Pier-Scouring Processes. *J. Eng. Mech.* **2016**, *142*, 06016005. [CrossRef]

15. Gazi, A.H.; Afzal, M.S. A new mathematical model to calculate the equilibrium scour depth around a pier. *Acta Geophys.* **2019**, *68*, 181–187. [CrossRef]
16. Gazi, A.H.; Purkayastha, S.; Afzal, M.S. The equilibrium scour depth around a pier under the action of collinear waves and current. *J. Mar. Sci. Eng.* **2020**, *8*, 36. [CrossRef]
17. Dey, S.; Raikar, R.V.; Roy, A. Scour at submerged cylindrical obstacles under steady flow. *J. Hydraul. Eng.* **2008**, *134*, 105–109. [CrossRef]
18. Zhao, M.; Cheng, L.; Zang, Z. Experimental and numerical investigation of local scour around a submerged vertical circular cylinder in steady currents. *Coast. Eng.* **2010**, *57*, 709–721. [CrossRef]
19. Euler, T.; Herget, J. Obstacle-Reynolds-number based analysis of local scour at submerged cylinders. *J. Hydraul. Res.* **2011**, *49*, 267–271. [CrossRef]
20. Zhao, M.; Zhu, X.; Cheng, L.; Teng, B. Experimental study of local scour around subsea caissons in steady currents. *Coast. Eng.* **2012**, *60*, 30–40. [CrossRef]
21. Baykal, C.; Sumer, B.M.; Fuhrman, D.R.; Jacobsen, N.G.; Fredsoe, J. Numerical investigation of flow and scour around a vertical circular cylinder. *Phil. Trans. R. Soc. A* **2014**, *373*, 20140104. [CrossRef]
22. Soulsby, R. *Dynamics of Marine Sands: A Manual for Practical Applications*; Thomas Telford: London, UK, 1997; 249p, Available online: http://www.vliz.be/en/imis?refid=85661 (accessed on 1 January 2021).
23. Sumer, B.M.; Christiansen, N.; Fredsøe, J. Time-scale of scour around a vertical pile. In Proceedings of the 2nd International Offshore and Polar Engineering Conference, San Francisco, CA, USA, 14–19 June 1992; Volume III, pp. 308–316. Available online: https://www.mendeley.com/catalogue/60d0bbdd-2ccb-3f63-95b4-93299e8a551f/ (accessed on 20 June 2016).
24. Du, S.T.; Liang, B.C. Comparisons of Local Scouring for Submerged Square and Circular Cross-Section Piles in Steady Currents. *Water.* **2019**, *11*, 1820. [CrossRef]
25. Cheng, N.S.; Zhao, K.F. Difference between static and dynamic angle of repose of uniform sediment grains. *Int. J. Sediment Res.* **2017**, *32*, 149–154. [CrossRef]
26. Tseng, M.H.; Yen, C.L.; Song, C.C.S. Computation of three-dimensional flow around square and circular piers. *Int. J. Numer. Meth. Fluids.* **2000**, *34*, 207–227. [CrossRef]